JOURNAL OF MATERIALS SCIENCE 26 (1991) 963–969

Microstructure of a rapidly solidified 65Al–20Cu–15Fe (at. %) alloy

PING LIU*
Department of Physics, Chalmers University of Technology, 412 96 Göteborg, Sweden
AN PANG TSAI, AKIHISA INOUE
Institute for Materials Research, Tohoku University, Sendai 980, Japan
L. ARNBERG
Swedish Institute for Metals Research, Drottning Kristinas väg 48, 114 28 Stockholm, Sweden

The microstructure of rapidly solidified 65Al–20Cu–15Fe (at.%) powders was investigated by analytical transmission electron microscopy. It was found that segregation in the powder particle occurred during solidification. The major phase present in the powder particles was the icosahedral quasicrystalline I-phase, which was determined to have space group $m\bar{3}\bar{5}$. Two other crystalline phases, β-$AlCu_3$ and θ-$Al_{13}Fe_4$, coexisted with the I-phase. The I-phase was revealed by convergent beam electron diffraction to have three-dimensional quasiperiodicity ($\tau = 1.618$) which is different from quasicrystals in the other systems. The compositions of the three phases have been analysed by energy dispersive X-ray analysis. The I-phase in this system could be approximately described as Al_5CuFe. The composition of the θ-$Al_{13}Fe_4$ was very close to the equilibrium condition while β-$AlCu_3$ was far from stoichiometry. An orientation relationship between β-$AlCu_3$ and θ-$Al_{13}Fe_4$ was found as follows:

$$[1\,1\,0]_\beta \parallel [0\,1\,0]_\theta$$
$$[1\,\bar{1}\,1]_\beta \parallel [0\,0\,1]_\theta$$

1. Introduction

Icosahedral phases with five-fold symmetry have been found in many alloy systems rapidly quenched from the melt [1, 2]. In a few systems, however, stable quasicrystals have been prepared by conventional solidification. Examples of these are Al–Li–Cu [3], Ga–Mg–Zn [4] and, more recently, Al–Cu–Fe [5]. Quasicrystals have been found in both melt-spun and arc-melted $Al_{65}Cu_{20}Fe_{15}$. These quasicrystals have been heat treated and found to be stable up to 0.98 T_m [5].

$Al_{65}Cu_{20}Fe_{15}$ has recently been rapidly solidified by high-pressure gas atomization. The aim of that experiment was to investigate the possibility of producing powder particles which are stable single quasicrystals. The present paper presents results from an analytical transmission electron microscopy investigation on the $Al_{65}Cu_{20}Fe_{15}$ powder particles.

2. Experimental procedure

The alloy was prepared by melting elemental aluminium, copper and iron. Powder was prepared by argon atomization in a high-pressure gas atomization apparatus [6].

Thin foils for transmission electron microscopy were prepared from powder size fractions which had been embedded in nickel deposited by electroplating [7]. The electrolyte used for the electroplating process had the following composition: 435 g/l $NiSO_4 \cdot 6H_2O$; 80 g/l $NiCl_4 \cdot 6H_2O$; 45 g/l H_3BO_3. The temperature was held constant at 50 °C and a current density of 2.4 mA cm^{-2} was used for the first 12 h followed by 9.6 mA cm^{-2} for 10 to 20 h. The deposition rate was about 1.9 μm h^{-1} for the latter step. Discs, 3 mm diameter, were punched from the resulting Al–Cu–Fe powder–Ni composite and jet electropolished in an electrolyte consisting of 25 vol % HNO_3 in methanol at 30 V and −30 °C. Occasionally a final thinning operation by ion-beam milling was used on these foils.

The thin foils were examined in a Jeol-2000FX scanning transmission electron microscope (TEM/STEM) which was equipped with a Link Systems AN-10000 energy dispersive X-ray (EDX) spectrometer and operated at 200 kV. The EDX results were made quantitative using the Link systems RTS 2/FLS computer program which compares spectra against stored standard peak profiles obtained from pure elements, applies the thin foil approximation [8] with experimental Kxsi values and corrects for absorption [9]. Specimen thicknesses were estimated using the contamination spot method [10].

3. Results

An optical micrograph of the cross-section of 65Al–20Cu–15Fe particles (in the size fraction of

* *Present address*: Research and Development Centre, AB Sandvik Steel, 811 81 Sandviken, Sweden.

0022–2461/91 $03.00 + .12

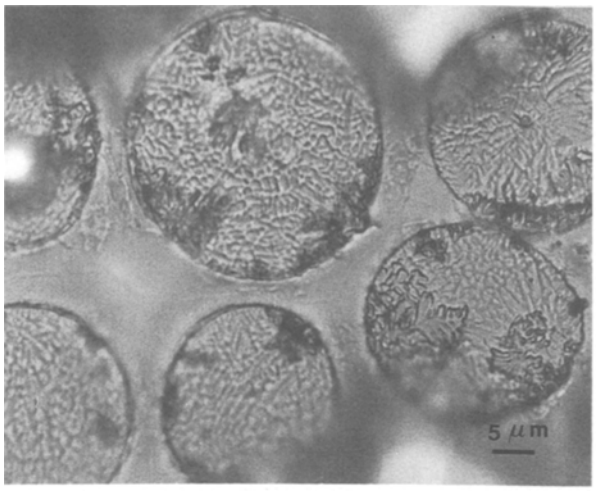

Figure 1 Optical micrograph of the cross-section of Al–Cu–Fe powder particles (size fraction of < 25 μm).

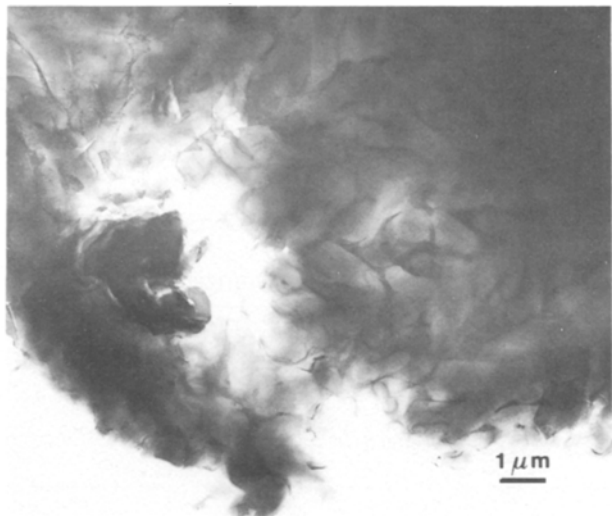

Figure 2 Transmission electron micrograph of rapidly solidified powder in the size range of < 25 μm diameter.

<25 μm) is shown in Fig. 1. It can be seen that each powder particle consists of several grains. The bright-field transmission microscopy image (BF) in Fig. 2 shows the microstructure of rapidly solidified 65Al–20Cu–15Fe powder particles in the size range <25 μm. It can be seen that the grains are equiaxed and have a size in the order of ~ 0.5 μm. Often the grains are featureless and have low contrast. Junctions between grains have often higher contrast.

Selected-area electron diffraction (SAED) patterns taken from the featureless grains show that these are the icosahedral quasicrystalline phase, I-phase [1]

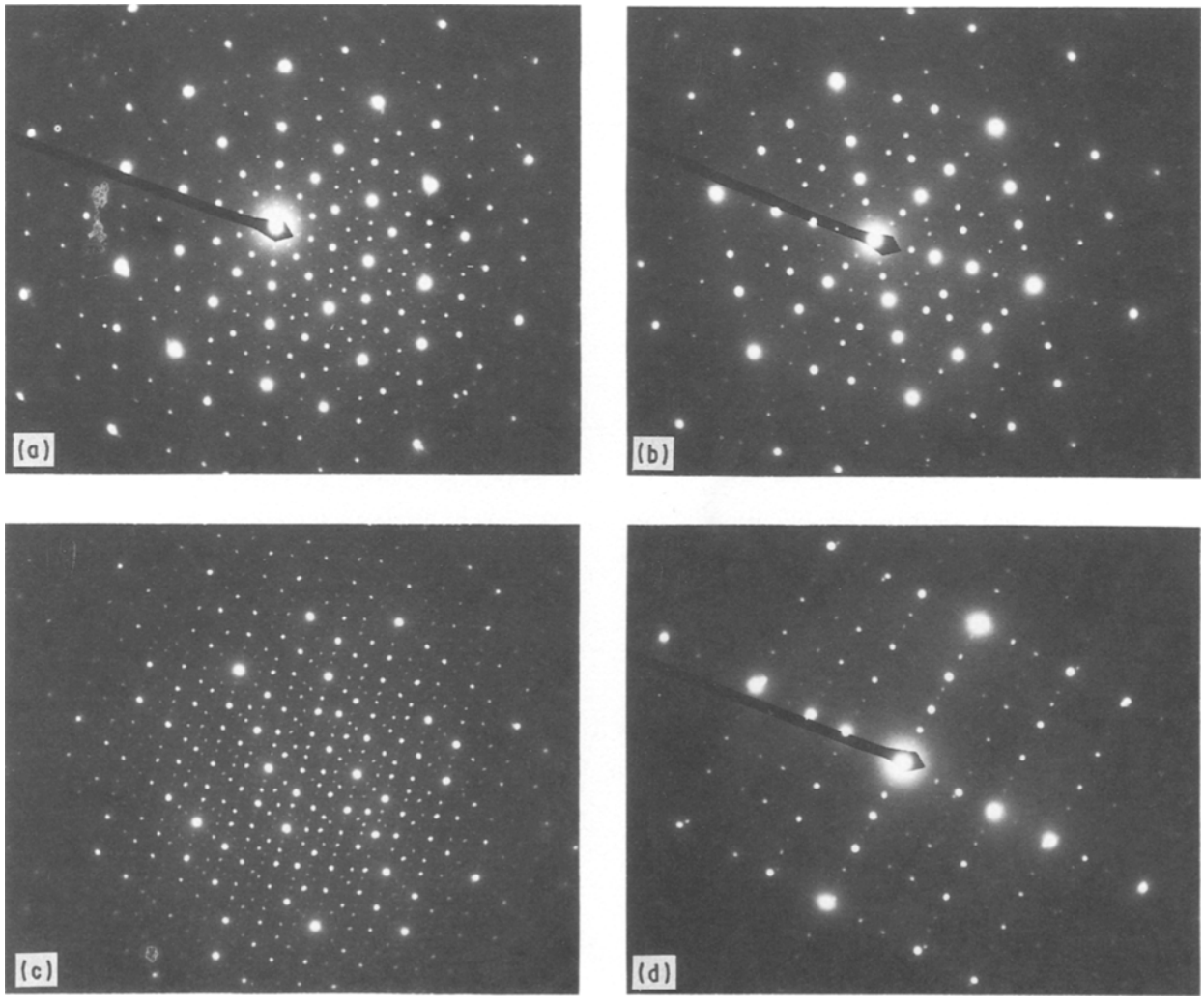

Figure 3 SAED patterns from the icosahedral quasicrystalline phase, I-phase. (a) Incident beam parallel to five-fold axis; (b) incident beam parallel to three-fold axis; (c) incident beam parallel to two-fold axis; (d) incident beam parallel to two-fold axis.

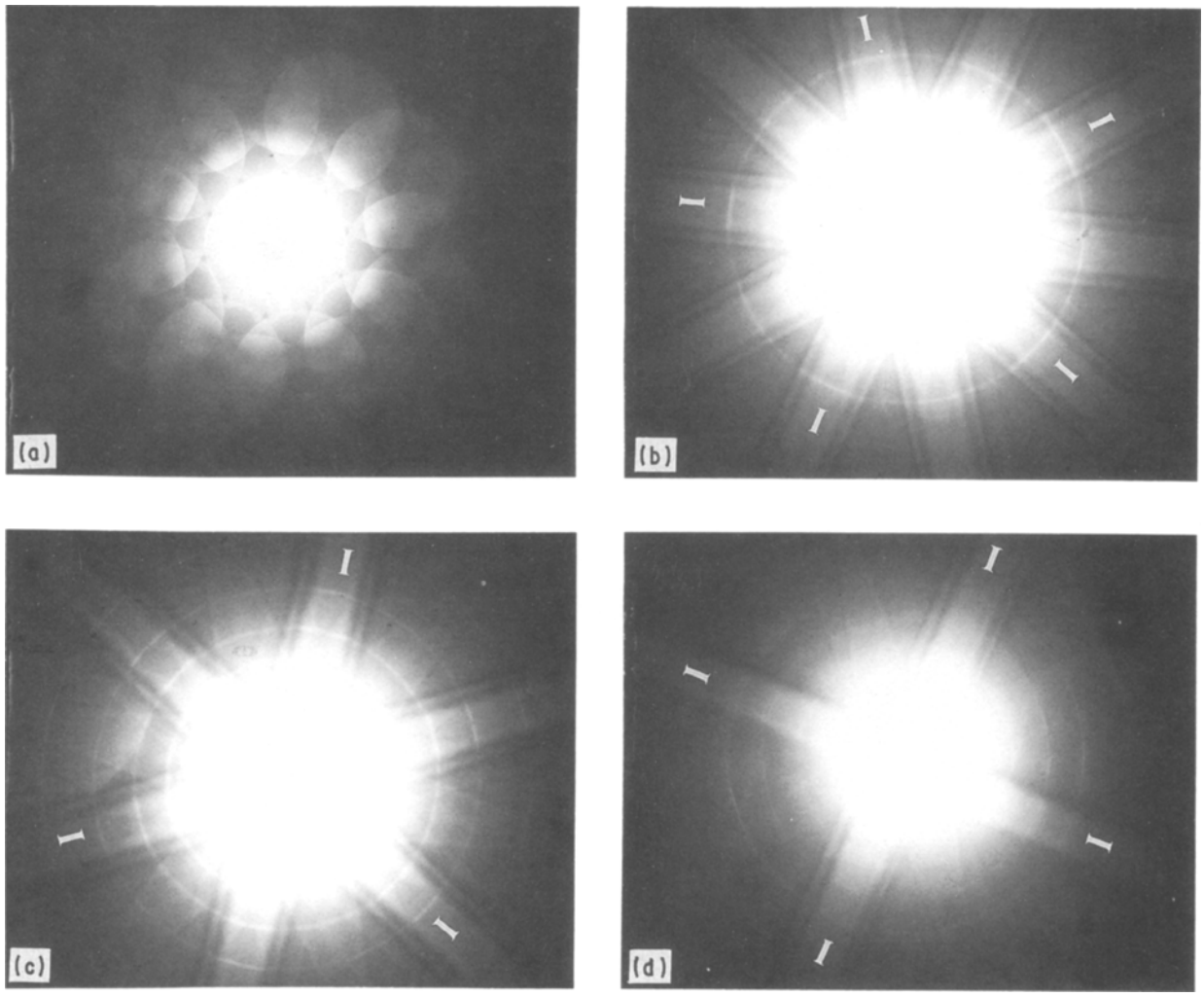

Figure 4 CBED patterns from the I-phase, which shows the Holz rings. (a, b) From five-fold axis corresponding to Fig. 3a, (a) zero-order Laue zone (ZOLZ), (b) higher-order Laue zone (HOLZ); (b) from three-fold axis corresponding to Fig. 3b; (c) from two-fold axis corresponding to Fig. 3c.

(see Fig. 3). Convergent beam electron diffraction patterns (CBED) from the I-phase are shown in Fig. 4. It can be seen that for the five-fold axis the whole pattern symmetry of the CBED is 5 m and for the three-fold axis it is 3 m [11]. Bendersky and Kaufman [12] summarized the diffraction groups of the three major zone axes for the two icosahedral point groups, i.e. 235 and $m\bar{3}\bar{5}$ [13]. From the CBED pattern symmetry for the diffraction groups [11], it is obvious that the point group for the I-phase can be readily determined by looking at its whole pattern (WP) symmetry in CBED from one of the three major zone axes. For the 235 group the WP symmetries for CBED from two-, three-, and five-fold zone axes are 2, 3 and 5, respectively. For the point group $m\bar{3}\bar{5}$, they are 2 mm, 3 m and 5 m, respectively. Therefore, the point group of the I-phase in the present material is $m\bar{3}\bar{5}$. Moreover, it is possible to make measurements of the spacings of the higher-order Laue zone (HOLZ) rings in the CBED patterns in Fig. 4. By applying the relationship between HOLZ

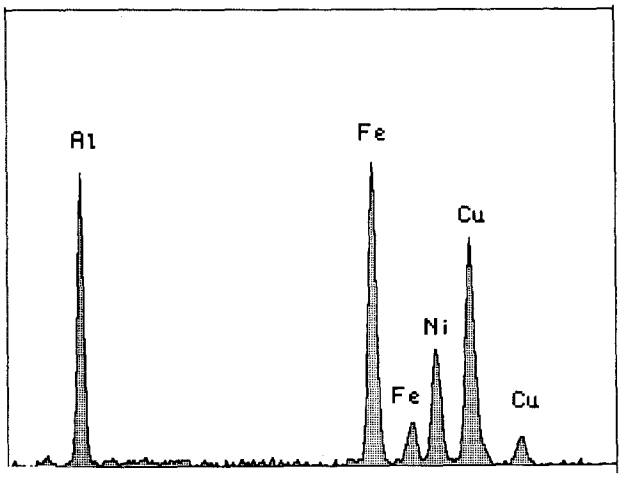

Figure 5 A typical EDX spectrum from the I-phase.

TABLE I Compositions of observed phases as determined by EDX (at. %)

Powder particle size (μm)		I-phase	β-$AlCu_3$	θ-$Al_{13}Fe_4$
< 25	Al	69.3 ± 0.9	49.5 ± 1.6	73.6 ± 0.3
	Cu	14.0 ± 0.9	44.3 ± 0.9	5.4 ± 0.1
	Fe	16.7 ± 0.8	6.2 ± 0.3	21.0 ± 0.3
25–37	Al	67.1 ± 0.9	50.0 ± 2.0	73.5 ± 0.2
	Cu	15.9 ± 1.3	47.2 ± 1.7	6.4 ± 0.6
	Fe	17.0 ± 0.9	2.8 ± 0.3	20.1 ± 0.5

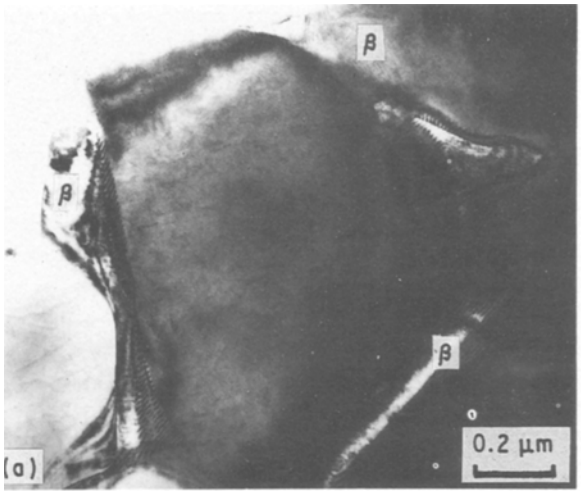

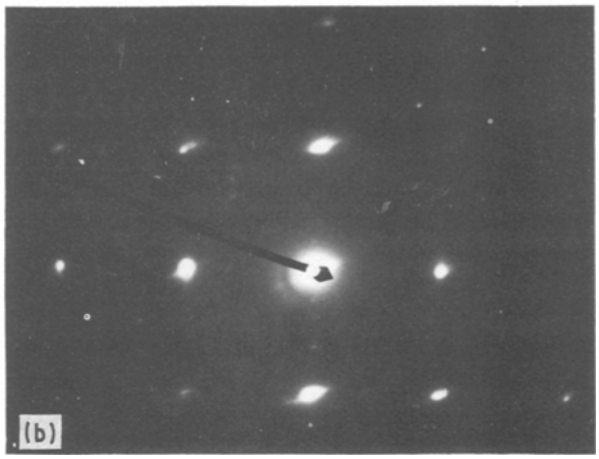

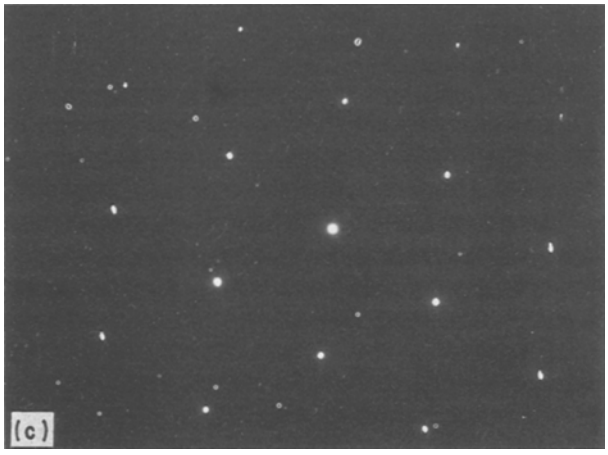

Figure 6 The β-$AlCu_3$ present in the junction of the I-phase grain boundaries. (a) Transmission electron micrograph; (b, c) SAED patterns from the β-$AlCu_3$, (b) ⟨1 0 0⟩ zone axis, (c) ⟨1 1 1⟩ zone axis.

rings and crystallographic parameters, the third dimension of the phase along the given zone axis can be determined [14, 15]. The results obtained indicated that the spacings of reciprocal lattice planes are non-periodic as expected for the quasiperiodic lattice of the icosahedral phase [1]. The spacings R_i (where i stands for the ith order Laue zone) of the first three reciprocal lattice planes normal to the beam direction, are $R_2/R_1 \simeq 1.27$ and $R_3/R_1 \simeq 1.62$ which give the quasiperiodicity in the real space $(R_2/R_1)^2 = \tau$ and $(R_3/R_1)^2 = \tau^2$ where τ is the golden mean $\tau = (1 + 5^{1/2})/2$, i.e. the characteristic number of icosahedral quasiperiodicity. A typical EDX spectrum from the I-phase is given in Fig. 5. It shows that the I-phase has higher iron content than the nominal alloy composition. The EDX analyses from a number of I-phase grains in several powder particles is given in Table I which gives the I-phase composition as approximately Al_5CuFe.

Fig. 6a shows the grain boundary phase. Moiré fringes of this phase can be seen. SAED patterns from the grain-boundary phase are shown in Fig. 6b. These could readily be indexed as ⟨1 1 1⟩ and ⟨1 0 0⟩ zone axes of a body-centred cubic phase with $a = 0.29$ nm. This phase was then determined as β-$AlCu_3$ which has the b c c crystal structure with space group Im3m [16]. Its lattice parameter is $a = 0.295$ nm but can vary with its composition, i.e. a decreases when the copper and/or iron content(s) increase [16].

Fig. 7 is a typical EDX spectrum from β-$AlCu_3$, which shows a great amount of copper and a very low iron content in comparison with the composition of the I-phase. The calculated composition from a number of EDX spectra is given in Table I.

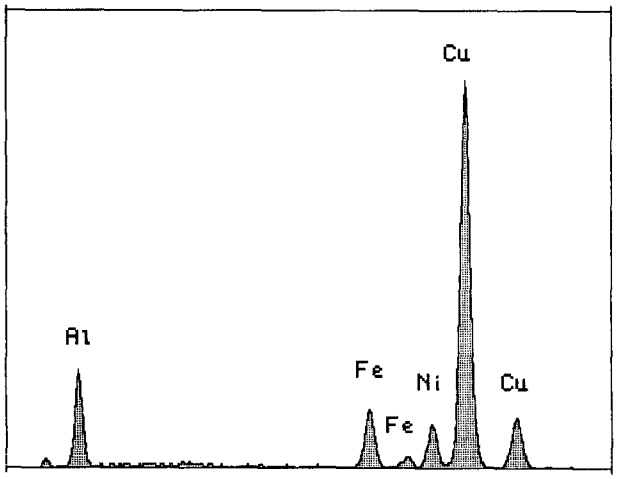

Figure 7 A typical EDX spectrum from the β-$AlCu_3$.

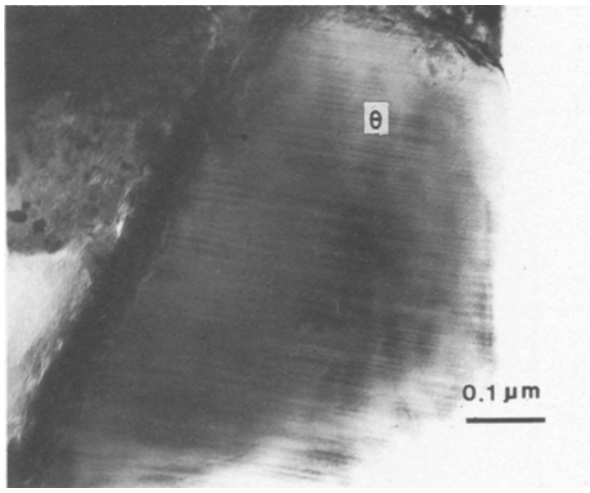

Figure 8 Transmission electron micrograph from the θ-$Al_{13}Fe_4$ grains.

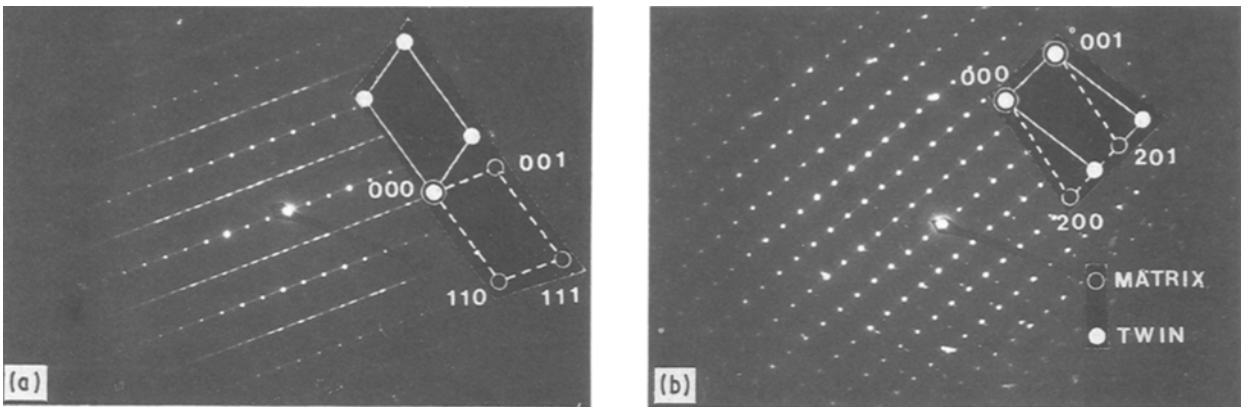

Figure 9 SAED patterns from the θ-$Al_{13}Fe_4$ and their schematic solutions. (a) From ⟨1 1 0⟩ zone axis; (b) from ⟨0 1 0⟩ zone axis.

Another type of grain can also be seen in Fig. 8. SAED patterns from this phase are shown in Fig. 9 from which the phase was identified as θ-$Al_{13}Fe_4$. This is an equilibrium phase and has a monoclinic structure [17]. The extra spots are due to twinning [17, 20] as shown by the schematic drawings and the streaking in the (0 0 1) has been reported to be due to microtwinning [18]. A typical EDX spectrum from this phase is given in Fig. 10. It shows a very high iron content and a low copper content. This is quite different from both the I-phase and β-$AlCu_3$. The EDX analyses of the phases are summarized in Table I and the crystal structure data are given in Table II.

When the selected-area aperture was placed over the β-$AlCu_3$ and θ-$Al_{13}Fe_4$ composite SAED patterns of the β-$AlCu_3$ and θ-$Al_{13}Fe_4$ could be obtained as shown in Fig. 11. This shows that the orientation relationship between the β-$AlCu_3$ and θ-$Al_{13}Fe_4$ is as follows

$$[1\,1\,0]_\beta \parallel [0\,1\,0]_\theta$$
$$[1\,\bar{1}\,1]_\beta \parallel [0\,0\,1]_\theta$$

The SAED patterns shown in Fig. 12 which are composite patterns from the β-$AlCu_3$ and I-phase show that an orientation relationship also exists between these two phases, but further work would be required in order to establish this correctly.

Observations, which were made on larger powder particles in the size range 25 to 37 μm, showed no major difference in the microstructure except that in the larger powder particles there was a slightly higher volume fraction of the crystalline phases, i.e. the β-$AlCu_3$ and θ-$Al_{13}Fe_4$ and a slightly higher content of iron in the β-$AlCu_3$ phase as shown in Table I.

4. Discussion

The results show that undercooling and cooling rate during solidification have not been sufficiently high to prevent segregation in powder particles. The existence of the β-$AlCu_3$ in the triple junction between the I-phase grains implied that the β-$AlCu_3$ formed after the solidification of the I-phase was completed. The melting temperature of the I-phase in this system is, therefore, probably higher than the β-$AlCu_3$ phase. This is different from the case of slow cooling in which

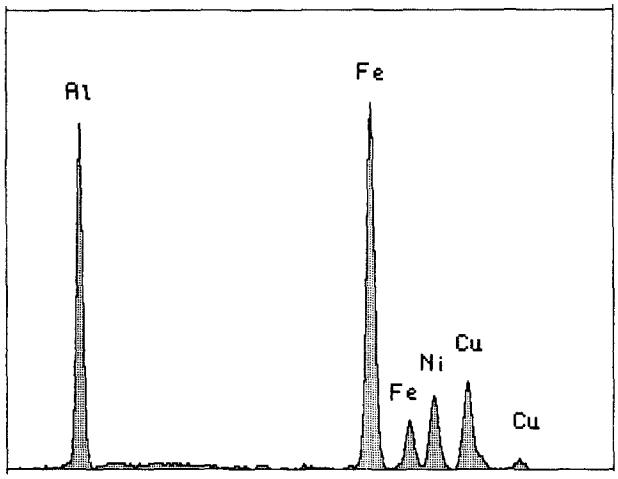

Figure 10 A typical EDX spectrum from the θ-$Al_{13}Fe_4$.

the I-phase was reported to have formed by a peritectic reaction between θ-$Al_{13}Fe_4$ and residual liquid [19]. The orientation relationship between the β-$AlCu_3$ and θ-$Al_{13}Fe_4$ indicates that a transformation reaction after solidification had taken place. The increase in the amount of iron dissolved in the β-$AlCu_3$ in smaller powder particles shown in Table I seems to be due to the higher cooling rate during solidification, but the total amount of iron and copper remained unchanged. The total contents of iron and copper in this phase were considerably higher than in the equilibrium case. However, EDX results show that the composition of the θ-$Al_{13}Fe_4$ in this alloy is very close to that of die-cast Al–Fe–Si alloys which forms during solidification at very low cooling rates [20]. The composition of the I-phase varied with the powder particle size, i.e. the cooling rate during solidification. The measured composition of this phase deviated from the nominal composition; the copper and iron contents were lower.

The contrast of the I-phase image in this system is very uniform irrespective of orientation. By comparison, the contrast of the I-phase in other alloy systems is generally considerably less uniform. This could be due to the lower stored energy in the I-phase in this system as noted by Tanaka *et al.* [21]. However, this point has yet to be proved.

TABLE II The structure data of observed phases

Phase	Space group	Lattice parameters (nm)	Reference
I-phase	Point group $m\bar{3}\bar{5}$		Present work
β-$AlCu_3$	Im3m	$a = 0.295$	[16]
θ-$Al_{13}Fe_4$	C2/m	$a = 1.549$ $b = 0.808$ $c = 1.247$ $\beta = 107°$	[17]

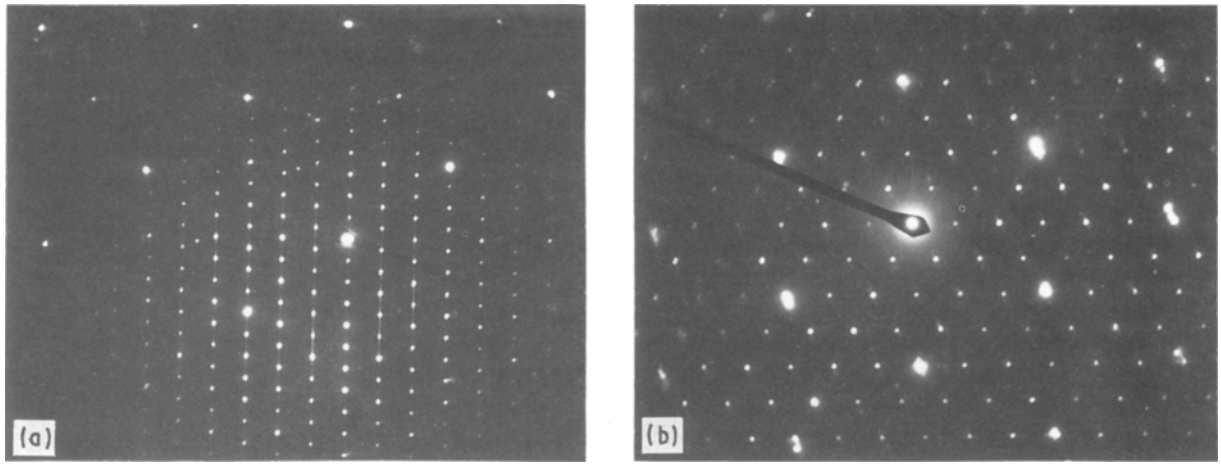

Figure 11 Composite SAED patterns of the β-$AlCu_3$ and θ-$Al_{13}Fe_4$. (a) $[1\,1\,0]_\beta \parallel [0\,1\,0]_\theta$; (b) $[1\,\bar{1}\,1]_\beta \parallel [0\,0\,1]_\theta$.

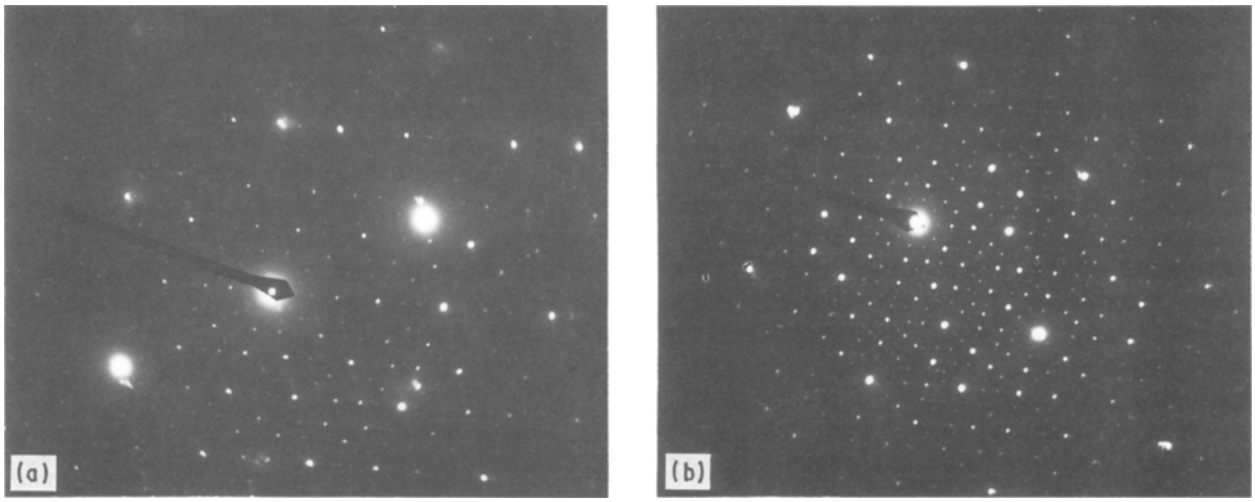

Figure 12 Composite SAED patterns of the θ-$Al_{13}Fe_4$ and I-phase. (a) $\langle 1\,1\,1\rangle_\beta \parallel$ 5-fold axis of the I-phase. (b) $\langle 1\,1\,1\rangle_\beta \parallel$ 2-fold axis of the I-phase.

I-phases in other alloy systems do not show three-dimensional quasiperiodicity. However, the present study of HOLZ rings in CBED patterns have shown that the I-phase in the rapidly solidified Al–Fe–Cu alloy shows three-dimensional quasiperiodicity, i.e. τ while in the other systems the two-dimensional quasiperiodicity is τ^3 [22].

5. Conclusions

1. Three phases have been observed in the rapidly solidified 65Al–20Cu–15Fe alloy, i.e. I-phase, β-$AlCu_3$ and θ-$Al_{13}Fe_4$.

2. The two crystalline phases, β-$AlCu_3$ and θ-$Al_{13}Fe_4$ precipitated after the formation of I-phase had completed.

3. An orientation relationship between the two crystalline phases has been found, i.e.

$$[1\,1\,0]_\beta \parallel [0\,1\,0]_\theta$$
$$[1\,\bar{1}\,1]_\beta \parallel [0\,0\,1]_\theta.$$

4. SAED and CBED from the I-phase show that the I-phase produced by rapidly solidified 65Al–20Cu–15Fe has a point group $m\bar{3}\bar{5}$.

5. The I-phase has been showed to have three-dimensional quasiperiodicity τ.

6. The composition of the I-phase has been determined by EDX to be approximately Al_5CuFe.

Acknowledgements

Encouragement and support from Professor G. L. Dunlop is gratefully acknowledged as is the assistance

for ion-beam thinning the specimens from Mr J. Yao. Financial support was received from the Swedish Board for Technical Development.

References

1. D. SHECHTMAN, I. BLECH, D. GRATIAS and J. W. CAHN, *Phys. Rev. Lett.* **53** (1984) 1951.
2. C. SURYANARAYANA and H. JONES, *Int. J. Rapid. Solid.* **3** (1987) 253.
3. P. SAINFORT, B. DUBOST and A. DUBUS, *C. R. Acad. Sci. (Paris)* **301** (1985) 689.
4. W. OHASHI and F. SPAEPEN, *Nature* **330** (1987) 555.
5. A. P. TSAI, A. INOUE and T. MASUMOTO, *Jpn J. Appl. Phys.* **26** (1987) L1505.
6. A. INOUE and T. MASUMOTO, T. EKIMOTO, S. FURUKAWA, Y. KURODA and H. S. CHEN, *Met. Trans.* **19A** (1988) 235.
7. R. BAUMANN and M. J. COOPER, in "Proceedings Metallographic-Tagung", Neu-Ulm, Germany, September 1984, edited by Dr Riederer (Verlag GmbH, Stuttgard, 1984).
8. G. CLIFF and G. W. LORIMER, *J. Microsc.* **103** (1975) 203.
9. G. WIRMARK, T. THORVALDSSON and H. NORDEN, in "Electron Microscopy and Analysis 1983", edited by P. Doig, Institute of Physics Conference Series no. 68 (Adam Hilger, Bristol, 1984) p. 71.
10. D. A. RAE, V. D. SCOTT and G. LOVE, in "Quantitative Microanalysis with High Spatial Resolution", consultant editors: G. W. Lovimer, M. H. Jacobs and P. Doig (The Metals Society, London, 1981) p. 57.
11. B. F. BUXTON, J. A. EADES, J. W. STEEDS and G. M. RACKHAM, *Phil. Trans. R. Soc.* **A281** (1976) 171.
12. L. A. BENDERSKY and M. J. KAUFMAN, *Phil. Mag.* **B53** (1986) L75.
13. T. HAHN (ed.), "International Tables for Crystallography", **A** (Reidel, Boston 1983).
14. J. W. STEEDS, in "Quantitative Electron Microscopy", edited by J. N. Chapman and A. J. Craven, Proceedings of the Twenty Fifth Scottish Universities Summer School in Physics, Glasgow, August 1982 (The Scottish University Summer School in Physics, Edinburgh, 1984) p. 49.
15. P. LIU, PhD thesis, Chalmers University of Technology (1986).
16. W. B. PEARSON (ed.), "A Handbook of Lattice Spacings and Structures of Metals and Alloys" (Pergamon Press, Oxford, 1964) pp. 139, 327.
17. P. J. BLACK, *Acta Crystallogr.* **8** (1955) 43.
18. P. SKJERPE, *Metall. Trans.* **18A** (1987) 189.
19. C. DONG, M. De BOISSIEU, J.-M. DDUBOIS, J. PANNETIER and C. JANOT, *J. Mater. Sci. Lett.* **8** (1989) 827.
20. P. LIU, T. THORVALDSSON and G. L. DUNLOP, *Mater. Sci. Technol.* **2** (1986) 1009.
21. M. TANAKA, M. TERAUCHI and T. KANEYAMA, "Convergent-Beam Electron Diffraction", Vol. 2 (Jeol Ltd, Tokyo, 1988) p. 91.
22. T. ISHIMASA, Y. FUKANO and M. TSUCHIMORI, *Phil. Mag. Lett.* **58** (1988) 157.

Received 11 September 1989
and accepted 19 February 1990